Fluid Dynamics & Materials Processing

Tech Science Press

DOI: 10.32604/fdmp.2024.053910

ARTICLE

Effect of Shrinkage Reducing Agent and Steel Fiber on the Fluidity and Cracking Performance of Ultra-High Performance Concrete

Yong Wan[1], Li Li[1], Jiaxin Zou[1], Hucheng Xiao[2], Mengdi Zhu[2], Ying Su[2] and Jin Yang[2,*]

[1]Wuhan Metro Bridge and Tunnel Management Co., Ltd., Wuhan, 430068, China

[2]School of Civil Engineering, Architecture and Environment, Hubei University of Technology, Wuhan, 430068, China

[*]Corresponding Author: Jin Yang. Email: jinyang@hbut.edu.cn

Received: 13 May 2024 Accepted: 08 July 2024 Published: 23 August 2024

ABSTRACT

Due to the low water-cement ratio of ultra-high-performance concrete (UHPC), fluidity and shrinkage cracking are key aspects determining the performance and durability of this type of concrete. In this study, the effects of different types of cementitious materials, chemical shrinkage-reducing agents (SRA) and steel fiber (SF) were assessed. Compared with M2-UHPC and M3-UHPC, M1-UHPC was found to have better fluidity and shrinkage cracking performance. Moreover, different SRA incorporation methods, dosage and different SF types and aspect ratios were implemented. The incorporation of SRA and SF led to a decrease in the fluidity of UHPC. SRA internal content of 1% (NSRA-1%), SRA external content of 1% (WSRA-1%), STS-0.22 and STE-0.7 decreased the fluidity of UHPC by 3.3%, 8.3%, 9.2% and 25%, respectively. However, SRA and SF improved the UHPC shrinkage cracking performance. NSRA-1% and STE-0.7 reduced the shrinkage value of UHPC by 40% and 60%, respectively, and increased the crack resistance by 338% and 175%, respectively. In addition, the addition of SF was observed to make the microstructure of UHPC more compact, and the compressive strength and flexural strength of 28 d were increased by 26.9% and 19.9%, respectively.

KEYWORDS

Ultra-high performance concrete; chemical shrinkage reducing agent; steel fiber; shrinkage cracking; repair and reinforcement

List of Abbreviations

UHPC	Ultra-high performance concrete
SRA	Shrinkage reducing agent
SF	Steel fiber
NSRA	SRA internal doping
WSRA	SRA external doping
CM	Cementitious material
S	Quartz sand
W	Water
PCE	Polycarboxylate Superplasticizers
STS	Straight steel fiber
STE	Hook steel fiber

1 Introduction

Ultra-high performance concrete (UHPC) is a novel type of cement-based composite material that has vast application prospects in the construction of basic infrastructure such as highways, bridges, and subway tunnels [1–3]. Compared with traditional concrete, it has outstanding compressive strength, toughness, and durability [4–6]. These performances are obtained by improving particle gradation [7,8], reducing or eliminating coarse aggregate [9], or adding steel fiber [10,11]. Due to the large amount of cementitious materials (more than 800 kg/m^3) and low water-binder ratio (W/B, less than 0.20), the fluidity and autogenous shrinkage of UHPC are significantly higher than those of conventional concrete, which leads to cracking of UHPC during difficult pumping and operation service period [12–14]. In particular, when UHPC is used under strong constraints, such as connections in concrete structures or steel joints in composite structures, the shrinkage of UHPC will lead to structural cracking and interface debonding, which endangers the mechanical qualities and endurance of the structure [15,16]. Therefore, it is of great significance to study the fluidity performance, shrinkage reduction and crack resistance of UHPC.

Cementitious material is the key factor determining the fluidity performance of UHPC [17–19]. The composition and type of cementitious materials are important parameters to adjust the fluidity of UHPC [20]. Jing et al. [21] used fly ash layer ball (FAC) as supplementary cementitious material (SCM) to prepare ultra-high performance concrete (UHPC). It was found that the 'ball bearing' and water-reducing effect of FAC particles significantly reduced the viscosity of UHPC slurry. Yan et al. [22] used waste glass powder to replace some cementitious materials, and the incorporation of glass powder (WGP) improved the fluidity of UHPC. Wu et al. [23] studied the effects of curing methods (standard curing, hot water curing and steam curing) on the mechanical performance of ultra-high performance concrete (UHPC) containing different supplementary cementitious materials (SCM) were investigated. The results show that the increase of GGBS or fly ash content has a limited or negative effect on the compressive strength of UHPC in terms of the type of curing system. According to the above research, it is found that the composition of the cementitious content has a great influence on the fluidity performance of UHPC.

In recent years, shrinkage-reducing admixtures (SRA) are commonly used to reduce the shrinkage of concrete [24]. SRA mainly alleviates the shrinkage stress by reducing the liquid-gas interfacial tension of the pore solution [25,26]. Bentz et al. [27] studied the early drying shrinkage of concrete with SRA, and found that SRA can effectively reduce the drying shrinkage of concrete, especially for cement-based materials with low water-cement ratio. Tang et al. [28] explored the effect of SRA on the shrinkage and creep of high-performance concrete. Studies have shown that SRA has a positive effect on reducing the shrinkage and creep deformation of concrete. Kong et al. [29] studied the effect of SRA on the shrinkage and mechanical performance of alkali-activated slag/fly ash-based mortars incorporating recycled fine aggregate. The results show that the addition of SRA can extend the crack initiation time by 14.6 times. After adding 3.0% SRA, the stress rate and crack width of mortar decreased by 74% and 91%, respectively. Masanaga et al. [30] developed a new type of shrinkage-reducing agent (N-SRA). The results show that N-SRA prolongs the time of shrinkage cracking of concrete under restricted conditions.

Steel fiber (SF) mainly forms a three-dimensional overlapping network inside the concrete to suppress shrinkage cracks [31,32]. Al-Kamyani et al. [33] studied the free shrinkage strain, constrained shrinkage strain and mechanical performance of seven (steel fiber reinforced concrete) SFRC mixtures. The results show that the free and constrained average shrinkage strains are very similar in all fiber blends, and they exhibit uneven shrinkage at the cross-sectional height. Feng et al. [34] studied the crack propagation behavior of hybrid steel fiber reinforced UHPC under bending load. When the substitution rate of longer fibers is higher, the crack initiation strain rate of the sample containing hybrid fibers decreases faster. Shen et al. [35] found that with the increase in the amount of SF at the double hook end, the cracking

risk of high-strength concrete decreased. When the amount of SF at the double hook end increased from 0% to 0.36%, the cracking parameters decreased by 62.4%, respectively.

Based on the above research, this paper explores the influence of different types of cementitious materials on the fluidity performance of UHPC, and deeply studies the influence of different mixing methods and contents of SRA and different types of SF on the shrinkage and cracking performance of UHPC. The effects of different types of cementitious materials, internal SRA, external SRA, 1% SRA content, 2% SRA content, straight steel fiber, end hook steel fiber and steel fiber aspect ratio on UHPC were systematically studied. The fluidity and mechanical performance of UHPC were characterized by fluidity, compressive strength, flexural strength and hydration heat tests. The shrinkage cracking behavior of UPHC was investigated by self-shrinkage and ring cracking tests. Finally, the microstructure of UHPC was characterized by scanning electron microscopy.

2 Raw Materials and Test Methods

2.1 Raw Materials

The M1, M2 and M3 cementitious materials used in this study were from Wuhan Huaxin Cement Co., Ltd. (Wuhan, China), Wuhan Sanyuan Special Building Materials Co., Ltd. (Wuhan, China) and China Communications Second Shipping Bureau Harbor New Materials Co., Ltd. Three different cementitious materials were shown in Fig. 1. The aggregate was quartz sand purchased from Wuhan, Hubei Province. The chemical shrinkage-reducing agent (SRA) was purchased from Wuhan. It was a light yellow liquid with a shrinkage reduction rate of about 40%. Steel fiber (SF) were straight type SF and end hook type SF, respectively. Two types of straight SF with aspect ratio (L/D) of 12.5/0.2 and 20/0.22 were selected, as shown in Table 1.

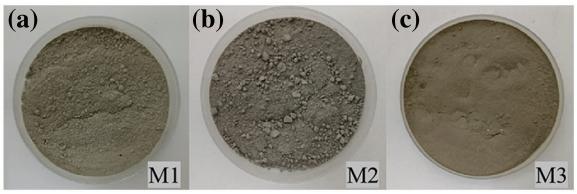

Figure 1: Three different types of cementitious materials. (a) M1 type cementitious material (b) M2 type cementitious material (c) M3 type cementitious material

Table 1: Basic parameters of steel fiber

Steel fiber type	Steel fiber size (L/D)
Short straight steel fiber	S-12.5/0.2
Long straight steel fiber	L-20/0.22
Short and hook steel fiber	S-22.4/0.29
Long and hook steel fiber	L-30/0.7

2.2 Mix Design

1) The mix proportion design of UHPC with different cementitious material systems

The ratio of cementitious material to sand in UHPC was 1.1. The stirring time was 8 min. The dosage of water reducing agent was 8‰. Three different cementitious materials based UHPC mixes are shown in Table 2.

Table 2: The mix proportion of three different cementitious materials UHPC

No.	CM/S	W/CM	PCE/‰
M1-UHPC	1.1	0.17	8
M2-UHPC	1.1	0.17	8
M3-UHPC	1.1	0.17	8

2) Mix proportion design of chemical shrinkage reducing agent (SRA) system UPHC

The chemical shrinkage-reducing agent (SRA) system UHPC mix is shown in Table 3. The incorporation of SRA was divided into two ways: SRA internal doping (NSRA) and SRA external doping (WSRA). The content of SRA was 1% and 2%.

Table 3: UHPC mix ratio of different blending methods and dosage SRA

No.	CM/g	S/g	W/g	PCE/g	SRA/%
Re	1000	909.1	175	9.5	0
NSRA-1%	1000	909.1	165	9.5	1
NSRA-2%	1000	909.1	155	9.5	2
WSRA-1%	1000	909.1	175	9.5	1
WSRA-2%	1000	909.1	175	9.5	2

Note: NSRA: SRA internal doping, WSRA: SRA external doping. CM: Cementitious material S: Quartz sand, W: Water, PCE: Polycarboxylate Superplasticizers, SRA: Shrinkage reducing agent.

3) Mix proportion design of steel fiber (SF) system UPHC

The UHPC mixes of different types and aspect ratio SF is shown in Table 4. The replacement rate of SF content was 5% of the mass of the cementitious material.

Table 4: Mix proportion design of steel fiber (SF) system UPHC

No.	CM/kg	S/kg	W/kg	Steel fiber type	Steel fiber/kg	PCE/‰
Re	18.9	17.1	3.31	–	–	8
STS-0.2	18.9	17.1	3.31	S-12.5/0.2	0.945	9
STS-0.22	18.9	17.1	3.31	L-20/0.22	0.945	9
STE-0.29	18.9	17.1	3.31	S-22.4/0.29	0.945	8
STE-0.7	18.9	17.1	3.31	L-30/0.7	0.945	8

Note: CM: Cementitious material S: Quartz sand, W: Water, PCE: Polycarboxylate Superplasticizers.

2.3 Specimen Preparation Methods

The forming method of the concrete block was carried out according to the Chinese standard GB/T 50080-2016. The paste test block was prepared according to the requirements of GB/T 8007-2000. All the test blocks were put into the standard curing room (temperature was 20°C, humidity was 95%) for 24 h, then the molds were removed and continued to be cured to the corresponding age for testing.

2.4 Test Methods

2.4.1 Compressive and Flexural Strength

The mechanical performance of the test blocks is in accordance with GB/T 17671-1999 [36]. In the flexural strength test, the size of the specimen was 40 mm × 40 mm × 160 mm, and the loading rate was set to 50 N/s. The block after the bending test should be immediately subjected to compression test. The broken half-cut test block was placed in the compression fixture, the direct compression surface was the side, and then placed on the press, the press was uniformly loaded at a rate of 2400N/s ± 200N/s until the specimen was destroyed.

2.4.2 Fluidity

The test method of fluidity followed the Chinese standard GB/T 2419-2005 [37].

2.4.3 Rheological

The RST-SST touch screen rheometer was used to test the rheological performance. Torque 100 mN·m. Torque resolution 0.15 μN·m. Speed range 0.01–1300 RPM.

2.4.4 Hydration Heat

Hydration heat was measured by TAM AIR thermal activity calorimeter. The experimental temperature was 20°C. Data were recorded every 10 s.

2.4.5 Ring Cracking

The ring cracking adopted YC-JY1581 ring type limiting shrinkage cracking strain acquisition instrument according to GB/T 50082-2009 [38]. The strain range of the instrument was 0 ± 30000 με. The data was collected by test instrument every 10 min. The temperature was maintained at 23°C ± 2°C and the humidity was 50% ± 5% RH.

2.4.6 Autogenous Shrinkage

Autogenous shrinkage performance test using contact shrinkage tester according to GB/T 50082-2009 [38]. Data were collected automatically every 10 min for 7 days.

2.4.7 Scanning Electron Microscope Test

The microstructure of the hardened paste was tested by FEI-Quanta FEG 450 electron microscope. The electron microscope works in high vacuum mode, with a working distance of about 10 mm, an acceleration voltage of 15 kV, and a magnification of 5–300000.

3 Results and Discussion

3.1 The Effect of Binders on the Performance of UHPC

3.1.1 Fluidity and Rheology Performance

Fig. 2 shows the effect of different types of cementitious materials on the fluidity performance of UHPC. From Fig. 2a, with the increase of slurry fluidity time, the fluidity performance of fresh slurry decreased gradually. The fluidity performance of M1-UHPC were 836, 812 and 794 mm at 30 s, 150 s and 30 min, respectively. When the time was the same, the fluidity performance of M1-UHPC was the largest. The possible reason was that the fly ash contained in the M1 cementitious material has a ball effect [39]. As shown in Fig. 2b, compared with M2-UPHC and M3-UPHC, the shear stress of M1-UPHC was the smallest. With the increase in shear rate, the shear stress of the slurry increased gradually. At the same shear rate, the shear stress of M3-UHPC was the largest. In general, the increase in shear stress meant the increase in slurry viscosity. As shown in Fig. 2c, the viscosities of M1-UPHC, M2-UPHC and M3-UHPC were 9637, 11273 and 12564 Pa·s, respectively. Compared with M1-UHPC, the viscosity of M2-UPHC and M3-UHPC were increased by 16.9% and 30.4%, respectively.

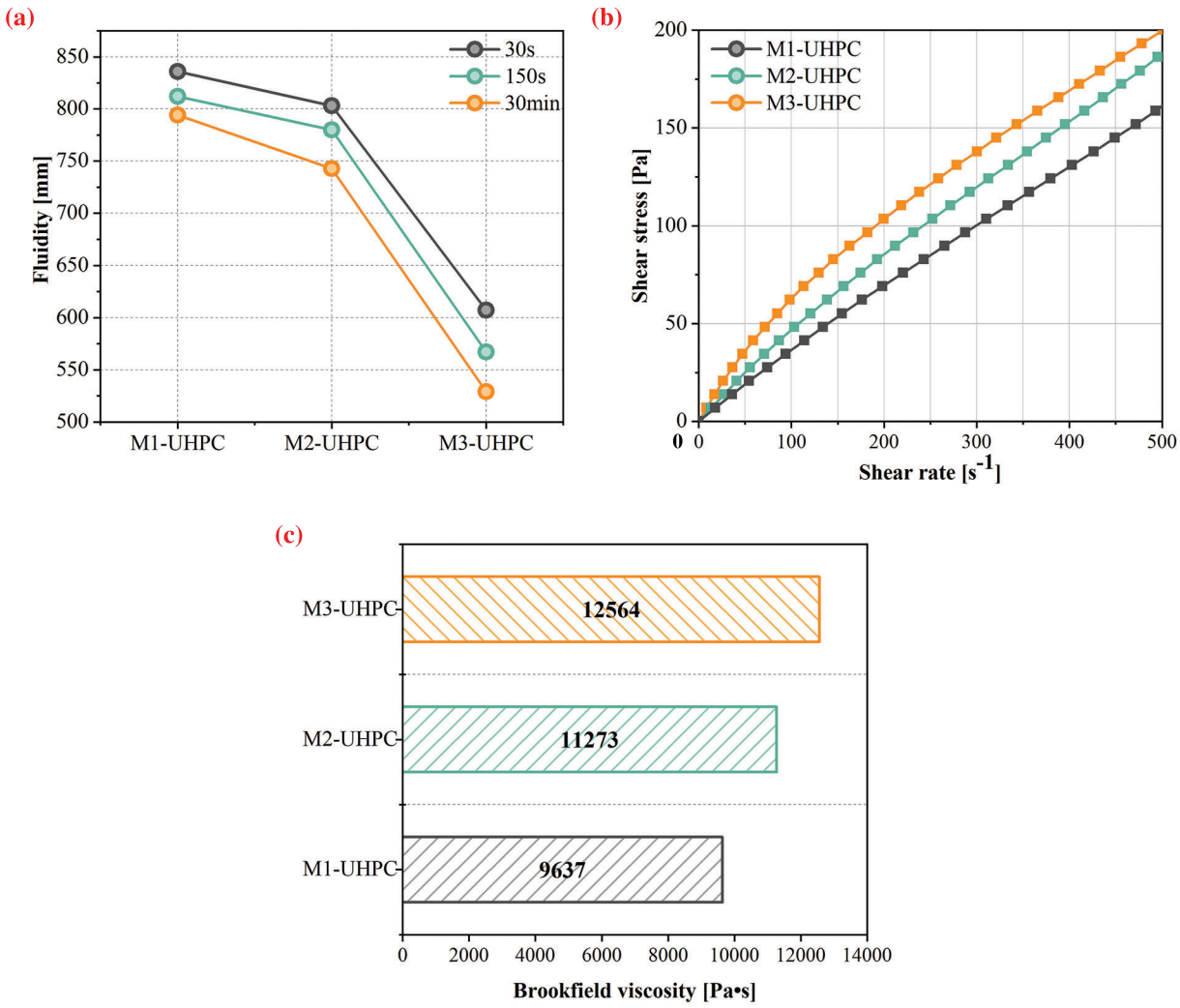

Figure 2: The effect of different cementitious materials on the fluidity performance of UHPC: (a) Fluidity; (b) Shear stress; (c) Brookfield viscosity

3.1.2 Mechanical Performance

Fig. 3 shows the influence of different cementitious materials on the compressive strength and flexural strength of UHPC. From Fig. 3a, the 3 d, 7 d and 28 d compressive strengths of M1-UHPC were 89.1, 107.8 and 118.8 MPa, respectively. Compared with M2-UHPC and M3-UHPC, the compressive strength of M1-UHPC was the largest at each age. The possible reason was that the particle size distribution of M1 cementitious materials was more uniform. Similar to the law of compressive strength, the flexural strength of UHPC with different cementitious materials also showed the same trend. As shown in Fig. 3b, when the age was 3 d, the flexural strength of UPHC of three different cementitious materials was almost the same. With the increase of curing time to 28 d, the flexural strength of M1-UHPC, M2-UHPC and M3-UHPC increased to 27.1, 25.9 and 25.3 MPa, respectively. It can be found that the flexural strength of M1-UPHC was the largest.

3.1.3 Autogenous Shrinkage and Cracking Performance

Autogenous shrinkage cracking performance is a key factor affecting the service performance of UPHC [40]. Fig. 4 shows the effects of different cementitious materials on the autogenous shrinkage and cracking

performance of UHPC. As shown in Fig. 4a, the contraction values of M1-UHPC, M2-UHPC and M3-UHPC were 161, 200 and 225 με, respectively. This indicated that the M1-UHPC was more conducive to reducing the shrinkage of UPHC. In general, the reduction of UHPC shrinkage will greatly prolong its cracking time. As shown in Fig. 4b, the cracking times of M1-UHPC, M2-UHPC and M3-UHPC were 13, 12 and 12 h, respectively. Compared with M2-UHPC and M3-UHPC, the cracking time of M1-UHPC was increased by 8%. Through the above research, it can be found that M1-UHPC was more conducive to the improvement of UPHC performance. The following research will be further studied on UPHC prepared by M1-UHPC.

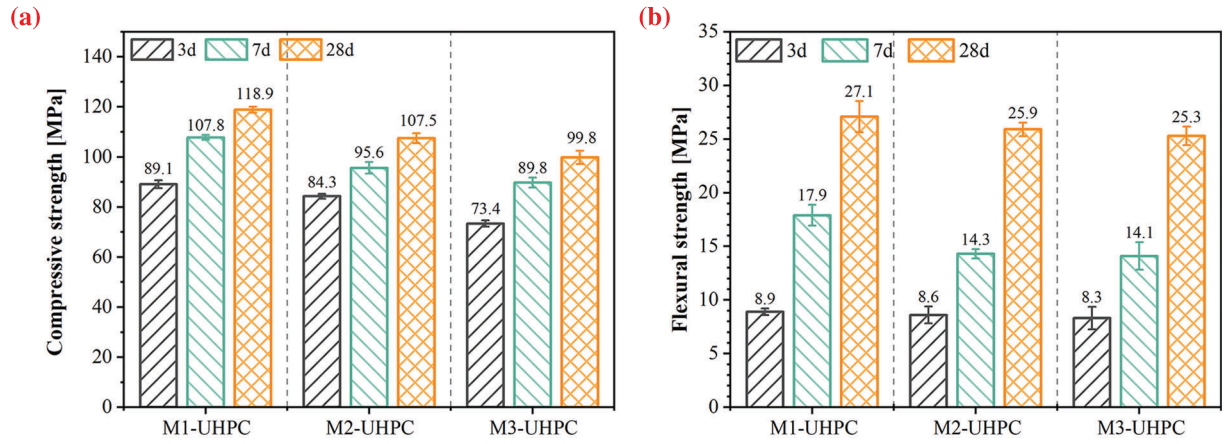

Figure 3: The influence of different cementitious materials on the compressive strength and flexural strength of UHPC: (a) Compressive strength (b) Flexural strength

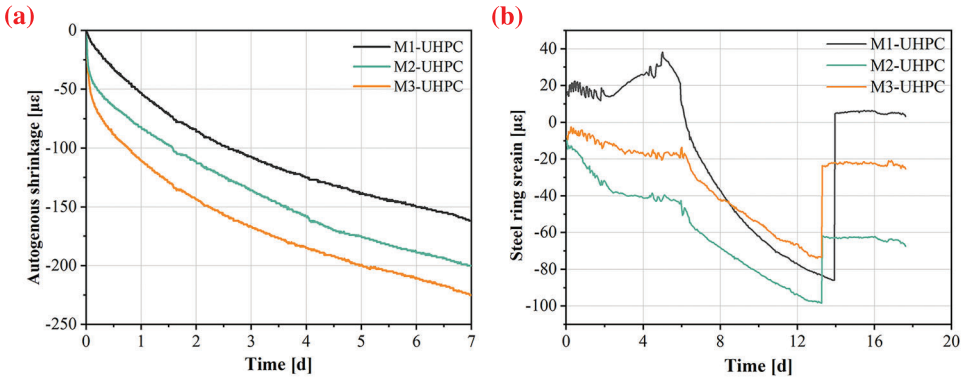

Figure 4: The effects of different cementitious materials on the autogenous shrinkage and cracking performance of UHPC: (a) Autogenous shrinkage (b) Cracking performance

3.2 The Effects of Chemical Shrinkage Reducing Agent and Steel Fiber on the Performance of UHPC

3.2.1 Fluidity Performance

The effects of SRA and SF on the working performance of UHPC are shown in Fig. 5. From Fig. 5a,b, it can be found that the fluidity performance of UHPC slurry decreased with the increase of SRA content. The fluidity performance of NSRA-1%, NSRA-2%, and NSRA-1% and WSRA-1%, decreased the fluidity performance of UHPC by 3.3% and 8.3%. The incorporation of SRA will reduce the fluidity performance of UHPC, which was mainly related to the chemical performance of SRA [41]. The addition of SRA

forms water content effect with other materials in UHPC, which will reduce the water content in the slurry and affect the fluidity performance of the slurry. Compared with NSRA, WSRA had little effect on the fluidity performance of UHPC. Compared with NSRA-1%, the fluidity performance of WSRA-1% was increased by 5.5%.

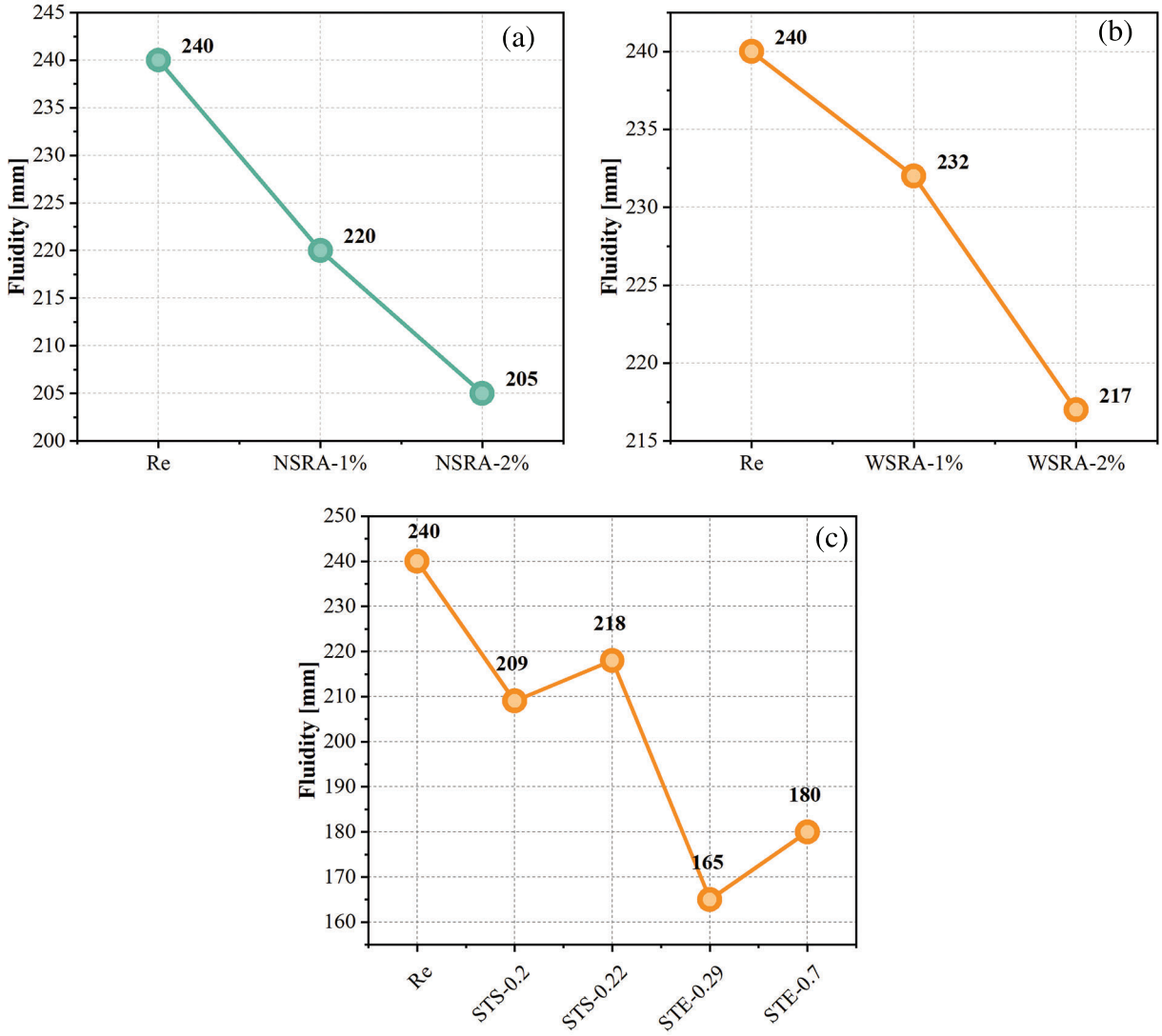

Figure 5: The effect of SRA and SF on UHPC working performance: (a) Fluidity performance of NSRA; (b) Fluidity performance of WSRA; (c) Fluidity performance of SF

Fig. 5c shows the effect of SF on the working performance of UHPC. From Fig. 5c, it can be found that the addition of SF significantly reduced the fluidity performance of UHPC slurry. Compared with straight SF, end-hook SF made the fluidity performance of slurry decrease more obviously. The reason was that the straight SF has a smooth surface, adding to the slurry will reduce the friction between the slurry. In addition, the aspect ratio of SF will also affect the fluidity of the slurry. The fluidity performance of STS-0.22 was 12 mm higher than that of STS-0.2. The fluidity of STE-0.7 was 15 mm

higher than that of STE-0.29. STS-0.22 and STE-0.7 decreased the fluidity performance of UHPC by 9.2% and 25%. This is because the higher the content of fine SF is, the easier it is for fibers to contact each other, and the easier it is to form fiber agglomeration, which will greatly reduce the fluidity performance of the slurry [42,43].

3.2.2 Mechanical Property

Fig. 6 shows the effects of SRA on the mechanical performance of UHPC. Compared with the control group, the addition of SRA decreased the compressive strength of UHPC, especially the early strength. NSRA-1% reduced the 3 d compressive strength by 2.5 MPa. Compared with NSRA, WSRA made the compressive strength and flexural strength of UHPC decrease more obviously. Compared with the control group, the compressive strength of NSRA-1%, NSRA-2%, WSRA-1% and WSRA-2% were decreased by 7.3%, 17.7%, 18.7% and 26.3%, respectively. This may be because the active substances in the chemical shrinkage-reducing agent will react with the cement in the concrete, resulting in the interference of the cement hydration process and reducing the strength of the concrete.

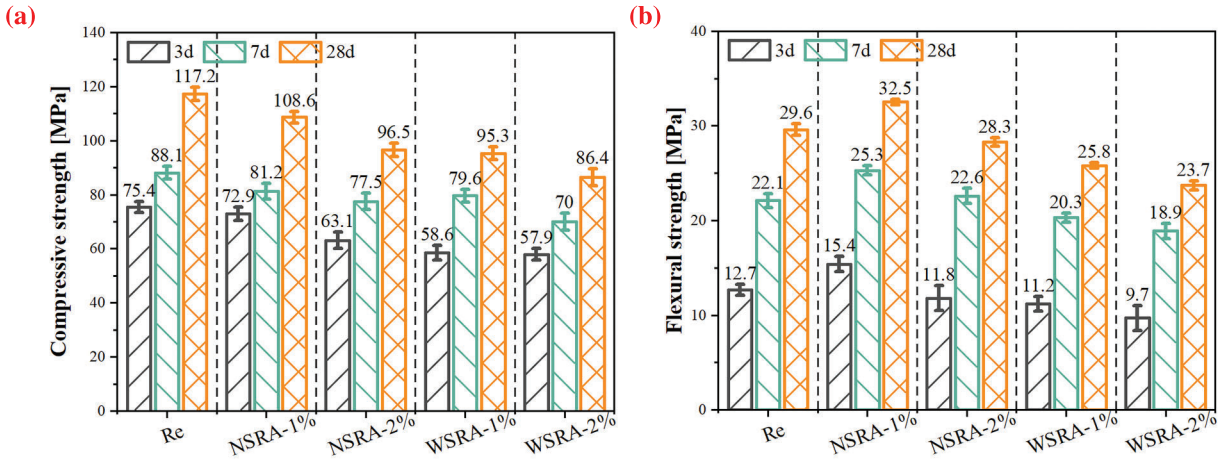

Figure 6: The effect of SRA on the mechanical performance of UHPC: (a) Compressive strength; (b) Flexural strength

Fig. 7 shows the effect of SF on the mechanical performance of UHPC. From Fig. 7, SF can effectively improve the compressive strength and flexural strength of UHPC. The end hook SF had the most obvious improvement on the compressive strength and flexural strength of UHPC. The 28 d compressive strength and flexural strength of STE-0.7 were 148.7 and 35.5 MPa, respectively, which were 26.9% and 19.9% higher than those of the blank group. With the decrease in SF aspect ratio, the compressive strength of UHPC decreased. The compressive strength of STE-0.29 was 136.5 MPa, which was 8.2% lower than that of STE-0.7. The 28 d compressive strength and flexural strength of STS-0.22 were 131.2 and 33.5 MPa, respectively, which were 11.9% and 13.1% higher than those of the blank group. With the decrease in the aspect ratio of straight SF, the compressive strength of UHPC also shows a decreasing trend. From Fig. 8, the addition of SF makes the UHPC structure denser, so that the compressive strength and flexural strength are enhanced. It can be found that steel fiber penetrates the internal structure of UHPC, which increases the flexural strength of UHPC. In addition, steel fiber can play a bridging role in UPHC, which can effectively reduce the defects and microcracks in the interfacial transition zone, thereby enhancing the overall performance of the material.

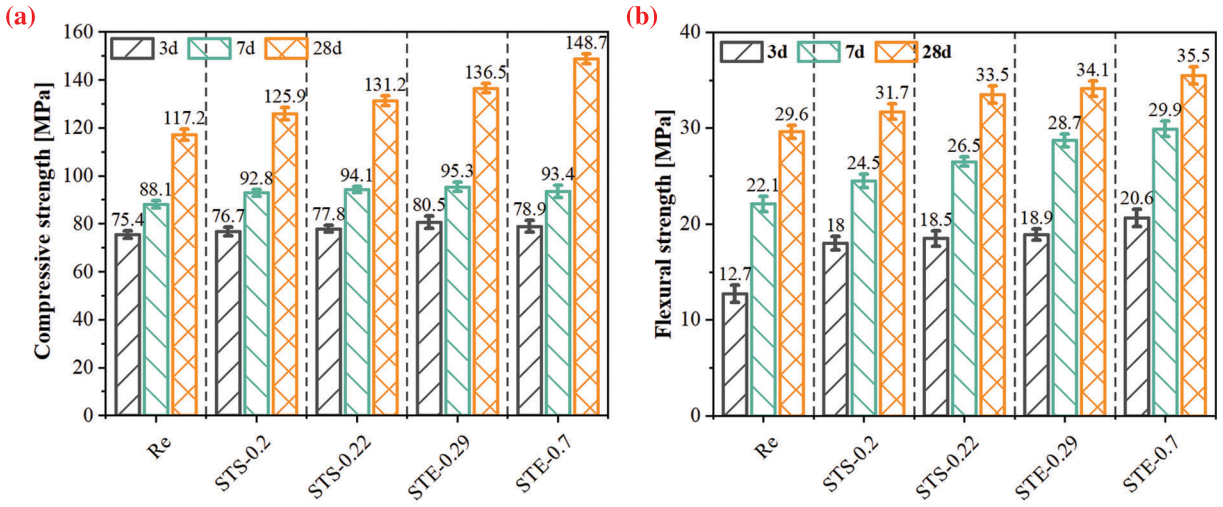

Figure 7: The effect of SF on the mechanical performance of UHPC: (a) Compressive strength; (b) Flexural strength

3.2.3 Hydration Heat

As a kind of polymer material, SRA will affect the hydration heat release of cement and materials when it is added to cement base [44]. In order to better evaluate the effect of SRA on the performance of UHPC, we tested the effect of SRA on the heat release performance of UHPC. Fig. 9 shows the effect of SRA on the hydration heat release of UHPC. From Fig. 9, it can be found that the hydration exothermic peak of UHPC shifts to the right and the peak decreases after the addition of SRA. This was because SRA affected the hydration process of cement, delayed the production of hydration product $Ca(OH)_2$, reduced the hydration of cement, and delayed the peak heat release. Compared with the control group, the hydration acceleration period of NSRA-1% and WSRA-1% was delayed 6.6 and 13.3 h, respectively. The use of SRA in UHPC effectively controls the temperature rise caused by hydration heat release, slows down the rate of cement hydration reaction, and reduces the temperature change and shrinkage stress of concrete. Comparing the two incorporation methods, it can be found that the NSRA-1% hydration exothermic peak is higher. From Fig. 9, the cumulative heat release of NSRA-1% was the highest, higher than that of WSRA-1%. which showed that NSRA-1% had little effect on the strength and hydration heat released performance of UHPC.

3.2.4 Autogenous Shrinkage

Fig. 10 shows the effect of SRA and SF on the shrinkage performance of UHPC. From Fig. 10a, the autogenous shrinkage of the control group was the largest, reaching nearly 500 με at 7d. SRA had a significant effect on the autogenous shrinkage of UHPC. Compared with WSRA, NSRA was more conducive to the shrinkage reduction of UHPC. NSRA-1% had the best shrinkage reduction effect, and the shrinkage value was 300 με, which was reduced by 40%. With the increase of SRA content, the shrinkage reduction effect decreases. The possible reason was that the excessive use of chemical shrinkage-reducing agents may lead to excessive reaction and cannot completely reduce the material, thus failing to achieve the desired shrinkage-reduction effect. Fig. 10b shows the effect of SF on the shrinkage performance of UHPC. It can be found that the addition of steel fiber significantly reduces the autogenous shrinkage of UHPC, and the shrinkage values of all test groups were smaller than that of the blank group. The shrinkage value of STE-0.7 was reduced by 60%, and the shrinkage value of STE-0.2 was reduced by 40%. It can be found that the end hook SF has a better shrinkage reduction effect than the straight SF, which was because the end hook steel fiber can increase the tensile strength and toughness of the concrete, thereby reducing the cracks caused by the shrinkage of the concrete.

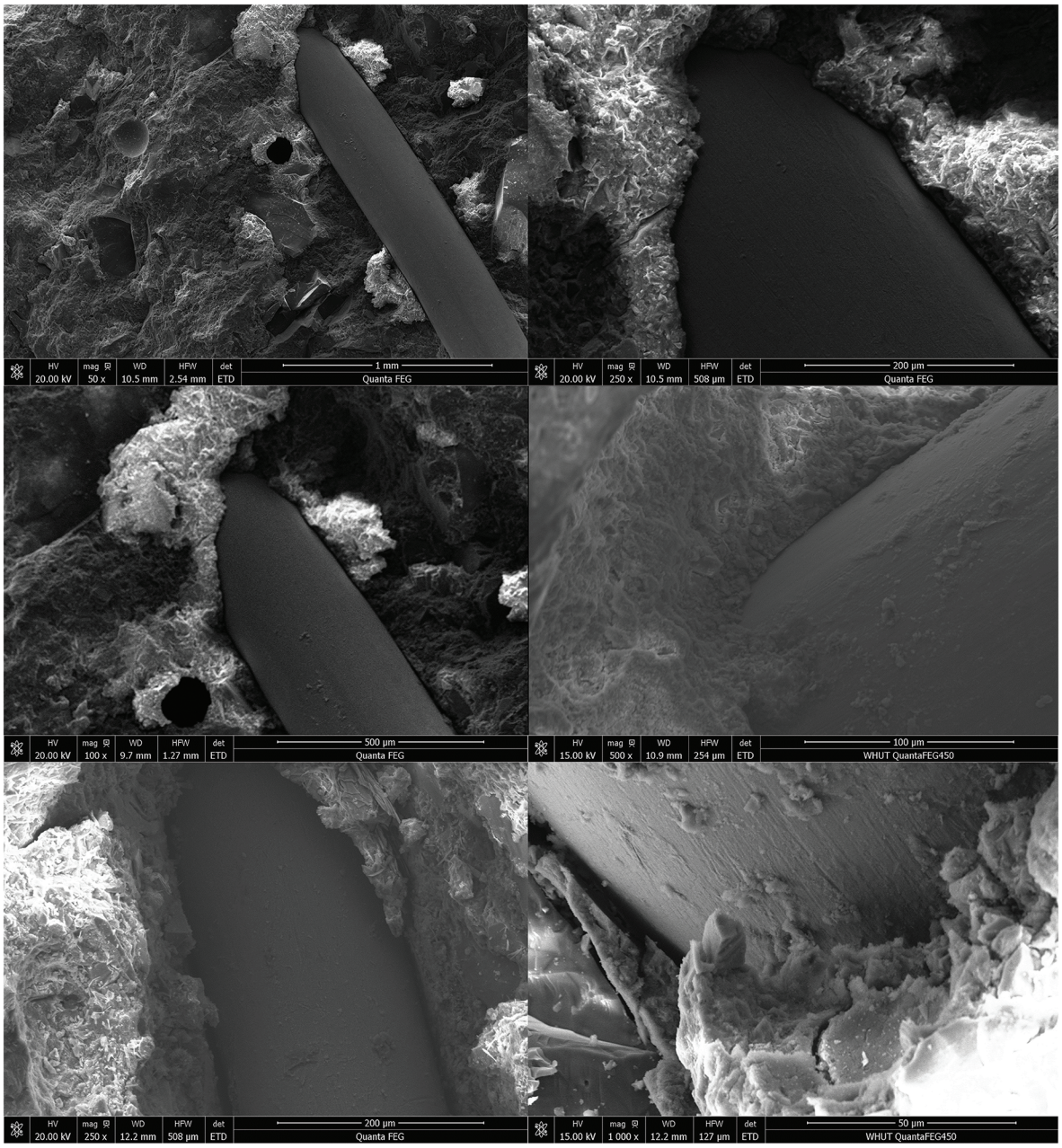

Figure 8: The effect of SF on the microstructure of UHPC

3.2.5 Cracking Performance

The effect of SRA and SF on the cracking performance of UHPC is shown in Fig. 11. From Fig. 11a, it can be found that the shrinkage-reducing agent has a significant effect on the cracking performance of UHPC. The control group was cracked at about 8 h. When SRA was incorporated, the cracking time of UHPC was significantly delayed. This was because SRA can slow down the evaporation of water, reduce the internal stress of concrete during hardening, and reduce the risk of ring cracking. The cracking time of NSRA-1% and WSRA-1% was 35 and 12 h, respectively, and the cracking resistance was improved by 338% and 50%, respectively, which indicated that the incorporation of SRA was more conducive to the improvement of UHPC cracking performance.

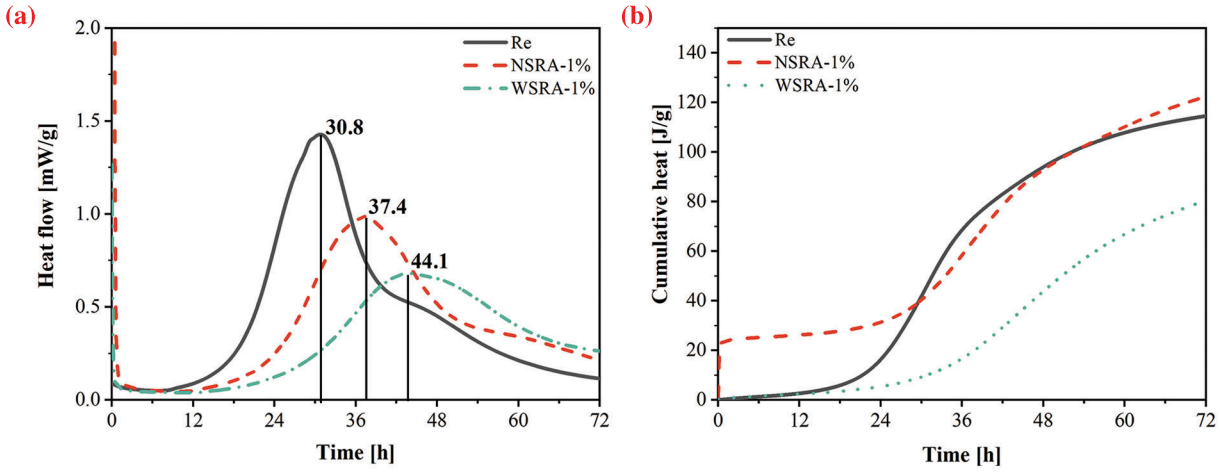

Figure 9: The effect of SRA on hydration heat release of UHPC: (a) Heat fluidity; (b) Cumulative heat

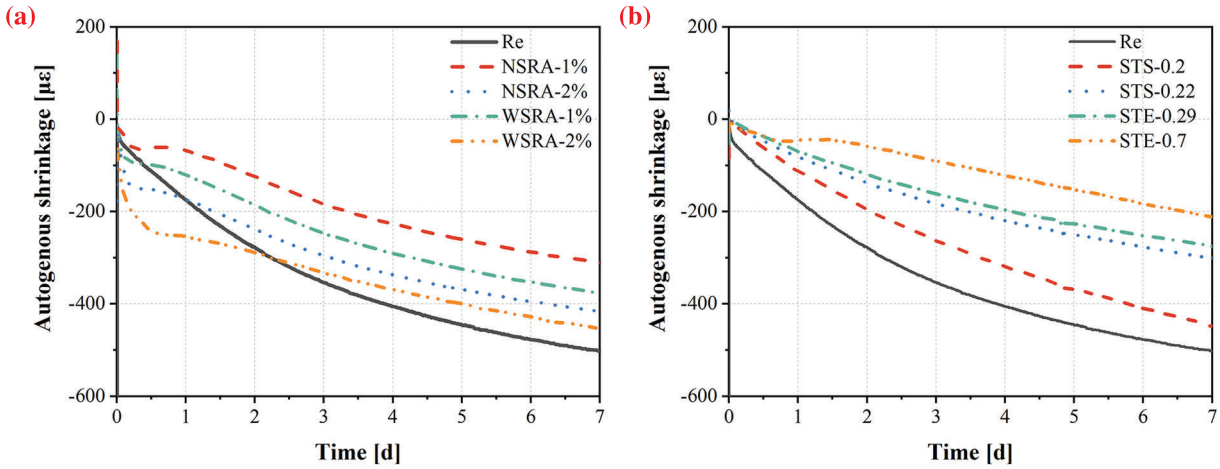

Figure 10: The effect of SRA and SF on the shrinkage performance of UHPC

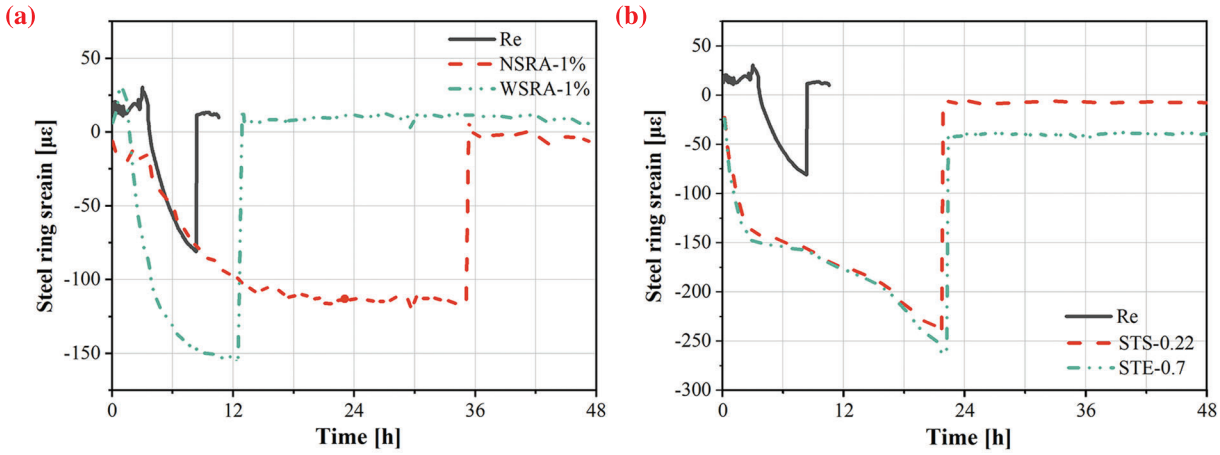

Figure 11: The effect of SRA and SF on the cracking performance of UHPC: (a) SRA; (b) SF

As a kind of material with high elastic modulus, steel fiber can significantly improve the crack resistance of concrete. From Fig. 11b compared with the control group, the incorporation of steel fiber improves the crack resistance of UHPC by nearly 175%. On the one hand, it was because steel fiber can cross the crack and form a bridge effect around it. On the other hand, steel fibers were dispersed in concrete and formed a network around the cracks, which limited the propagation of cracks and reduced the length and width of cracks. Compared with STS-0.22, STE-0.7 was more conducive to the improvement of the cracking performance of UPHC. This was mainly because the end hook steel fiber can effectively resist the external tension, and reduce the tension of the concrete itself, thus delaying the cracking time of UPHC.

4 Conclusions

In this paper, the effects of different types of cementitious materials, different mixing methods and dosages of SRA, different types and dosages of SF on the shrinkage and cracking performance of UHPC were systematically explored. The following conclusions are drawn:

(1) Compared with M1-UHPC, the viscosity of M2-UHPC and M3-UHPC were increased by 16.9% and 30.4%, respectively. The M1-UHPC showed good fluidity performance.

(2) The shrinkage and cracking performance of M1-UHPC were more excellent. the shrinkage values of M1-UHPC, M2-UHPC and M3-UHPC were 161, 200 and 225 με, respectively. Compared with M2-UHPC and M3-UHPC, the cracking time of M1-UHPC was increased by 8%.

(3) The incorporation of SRA and SF will reduce the fluidity of UHPC. The effect of SRA and SF on the fluidity of UHPC was more obvious.

(4) The incorporation of SRA had a negative impact on the working performance of UHPC. The compressive strength of SRA internal content of 1% (NSRA-1%) and SRA external content of 1% (WSRA-1%) were decreased by 7.3% and 18.7%, respectively. The addition of SF was beneficial to the densification of UHPC structure. The 28 d compressive strength and flexural strength of STE-0.7 were increased by 26.9% and 19.9%, respectively.

(5) SRA slowed down the early hydration rate of UHPC. The hydration acceleration period of NSRA-1% and WSRA-1% were delayed by 6.6 and 13.3 h. Compared with WSRA-1%, NSRA-1% had more cumulative heat release.

(6) The incorporation of SRA and SF improved the shrinkage cracking performance of UHPC. NSRA-1% and STE-0.7 had the best shrinkage reduction effect, which reduced the shrinkage value by 40% and 60%, respectively. NSRA-1% and STE-0.7 improved the crack resistance of UHPC by 338% and 175%, respectively.

Acknowledgement: The authors express their gratitude to the editors and reviewers for their insightful comments that helped to raise the caliber of our manuscript.

Funding Statement: The authors would like to acknowledge the Key Research and Development Program of Hubei Province (2022BCA082 and 2022BCA077).

Author Contributions: The authors confirm contribution to the paper as follows: study conception and design: Yong Wan, Li Li, Jin Yang; data collection: Ying Su, Jin Yang; analysis and interpretation of results: Yong Wan, Li Li, Jiaxin Zou, Mengdi Zhu; draft manuscript preparation: Yong Wan, Hucheng Xiao, Jin Yang. All authors reviewed the results and approved the final version of the manuscript.

Availability of Data and Materials: The data used to support the findings of this study are available from the corresponding author upon request.

Ethics Approval: Not applicable.

Conflicts of Interest: The authors declare that they have no conflicts of interest to report regarding the present study.

References

1. Ngo TT, Park JK, Pyo S, Kim DJ. Shear resistance of ultra-high-performance fiber-reinforced concrete. Constr Build Mater. 2017;151:246–57.
2. Sohail MG, Kahraman R, Al Nuaimi N, Gencturk B, Alnahhal W. Durability characteristics of high and ultra-high performance concretes. J Build Eng. 2021;33:101669.
3. Pereira Prado L, Carrazedo R, Khalil El Debs M. Interface strength of high-strength concrete to ultra-high-performance concrete. Eng Struct. 2022;252:113591.
4. Abdellatief M, Elrahman MA, Abadel AA, Wasim M, Tahwia A. Ultra-high performance concrete versus ultra-high performance geopolymer concrete: mechanical performance, microstructure, and ecological assessment. J Build Eng. 2023;79:107835.
5. Tarasov VV, Aptukov VN, Pestrikova VS. Deformation and failure of concrete lining in vertical shaft at intersections with horizontal tunnels. J Min Sci. 2021;56(5):726–31.
6. Alsalman A, Dang CN, Micah Hale W. Development of ultra-high performance concrete with locally available materials. Constr Build Mater. 2017;133:135–45. doi:10.1016/j.conbuildmat.2016.12.040.
7. Li PP, Yu QL, Brouwers HJH. Effect of coarse basalt aggregates on the properties of ultra-high performance concrete (UHPC). Constr Build Mater. 2018;170:649–59. doi:10.1016/j.conbuildmat.2018.03.109.
8. Ahmed Sbia L, Peyvandi A, Soroushian P, Balachandra AM, Sobolev K. Evaluation of modified-graphite nanomaterials in concrete nanocomposite based on packing density principles. Constr Build Mater. 2015;76:413–22. doi:10.1016/j.conbuildmat.2014.12.019.
9. LS L, NT L, ZH G, ZM Y. Experimental research on dynamic mechanics of early age concrete. J Min Sci Technol. 2020;5(5):502–10.
10. Yoo DY, Kim S, Kim JJ, Chun B. An experimental study on pullout and tensile behavior of ultra-high-performance concrete reinforced with various steel fibers. Constr Build Mater. 2019;206:46–61. doi:10.1016/j.conbuildmat.2019.02.058.
11. Kim JJ, Yoo DY, Banthia N. Benefits of curvilinear straight steel fibers on the rate-dependent pullout resistance of ultra-high-performance concrete. Cem Concr Compos. 2021;118:103965.
12. Liu Q, Wang Y, Sun C, Cheng S, Yang C. Carbon sequestration and mechanical properties of foam concrete based on red mud pre-carbonation and CO_2 foam bubbles. Constr Build Mater. 2024;426:135961.
13. Kheir J, Klausen A, Hammer TA, De Meyst L, Hilloulin B, Van Tittelboom K, et al. Early age autogenous shrinkage cracking risk of an ultra-high performance concrete (UHPC) wall: modelling and experimental results. Eng Fract Mech. 2021;257:108024.
14. Zhang M, Fang K, Wang D, Yao G, Liu Z, Li H. Study on compatibility of fresh cement paste mixed with modified coal gasification slag and superplasticizer. J Min Sci Technol. 2021;6(6):737–45.
15. Ghafari E, Ghahari SA, Costa H, Júlio E, Portugal A, Durães L. Effect of supplementary cementitious materials on autogenous shrinkage of ultra-high performance concrete. Constr Build Mater. 2016;127:43–8.
16. Hisseine OA, Soliman NA, Tolnai B, Tagnit-Hamou A. Nano-engineered ultra-high performance concrete for controlled autogenous shrinkage using nanocellulose. Cem Concr Res. 2020;137:106217.
17. Zhou H, Zhu H, Gou H, Yang Z. Comparison of the hydration characteristics of ultra-high-performance and normal cementitious materials. Materials. 2020;13(11):2594.
18. Mousavinezhad S, Gonzales GJ, Toledo WK, Garcia JM, Newtson CM, Allena S. A comprehensive study on nonproprietary ultra-high-performance concrete containing supplementary cementitious materials. Materials. 2023;16(7):2622.
19. Wu YY, Zhang J, Liu C, Zheng Z, Lambert P. Effect of graphene oxide nanosheets on physical properties of ultra-high-performance concrete with high volume supplementary cementitious materials. Materials. 2020;13(8):1929.

20. Lin Y, Yan J, Wang Z, Fan F, Zou C. Effect of silica fumes on fluidity of UHPC: experiments, influence mechanism and evaluation methods. Constr Build Mater. 2019;210:451–60.
21. Jing R, Liu Y, Yan P. Uncovering the effect of fly ash cenospheres on the macroscopic properties and microstructure of ultra high-performance concrete (UHPC). Constr Build Mater. 2021;286:122977.
22. Yan P, Chen B, Zhu M, Meng X. Study on mechanical properties and microstructure of green ultra-high performance concrete prepared by recycling waste glass powder. J Build Eng. 2024;82:108206. doi:10.1016/j.jobe.2023.108206.
23. Wu Z, Shi C, He W. Comparative study on flexural properties of ultra-high performance concrete with supplementary cementitious materials under different curing regimes. Constr Build Mater. 2017;136:307–13. doi:10.1016/j.conbuildmat.2017.01.052.
24. Ferdosian I, Camões A. Mechanical performance and post-cracking behavior of self-compacting steel-fiber reinforced eco-efficient ultra-high performance concrete. Cem Concr Compos. 2021;121:104050.
25. Wang X, Yang W, Ge Y, Feng D. The influence of shrinkage-reducing agent solution properties on shrinkage of cementitious composite using grey correlation analysis. Constr Build Mater. 2020;264:120194.
26. Kalina L, Bílek V, Bartoníčková E, Kalina M, Hajzler J, Novotný R. Doubts over capillary pressure theory in context with drying and autogenous shrinkage of alkali-activated materials. Constr Build Mater. 2020;248:118620. doi:10.1016/j.conbuildmat.2020.118620.
27. Bentz DP, Geiker MR, Hansen KK. Shrinkage-reducing admixtures and early-age desiccation in cement pastes and mortars. Cem Concr Res. 2001;31(7):1075–85. doi:10.1016/S0008-8846(01)00519-1.
28. Tang C, Dong R, Tang Z, Long G, Zeng X, Xie Y, et al. Effects of shrinkage reducing admixture and internal curing agent on shrinkage and creep of high performance concrete. J Build Eng. 2023;71:106446. doi:10.1016/j.jobe.2023.106446.
29. Kong F, Xu F, Xiong Q, Xu S, Li X, Fu W, et al. Experimental research on properties of UHPC based on composite cementitious materials system. Coatings. 2022;12(8):1219.
30. Masanaga M, Hirata T, Kawakami H, Morinaga Y, Nawa T, Elakneswaran Y. Effects of a New type of shrinkage-reducing agent on concrete properties. Materials. 2020;13(13):3018. doi:10.3390/ma13133018.
31. Choi JS, Lee HJ, Yuan TF, Yoon YS. Mechanical and shrinkage performance of steel fiber reinforced high strength self-compacting lightweight concrete. Cem Concr Compos. 2023;144:105296. doi:10.1016/j.cemconcomp.2023.105296.
32. Shin W, Yoo DY. Influence of steel fibers corroded through multiple microcracks on the tensile behavior of ultra-high-performance concrete. Constr Build Mater. 2020;259(7):120428. doi:10.1016/j.conbuildmat.2020.120428.
33. Al-Kamyani Z, Figueiredo FP, Hu H, Guadagnini M, Pilakoutas K. Shrinkage and flexural behaviour of free and restrained hybrid steel fibre reinforced concrete. Constr Build Mater. 2018;189:1007–18. doi:10.1016/j.conbuildmat.2018.09.052.
34. Feng Z, Shen D, Luo Y, Huang Q, Liu Z, Jiang G. Effect of polypropylene fiber on early-age properties and stress relaxation of ultra-high-performance concrete under different degrees of restraint. J Build Eng. 2023;68:106035. doi:10.1016/j.jobe.2023.106035.
35. Shen D, Kang J, Yi X, Zhou L, Shi X. Effect of double hooked-end steel fiber on early-age cracking potential of high strength concrete in restrained ring specimens. Constr Build Mater. 2019;223:1095–105. doi:10.1016/j.conbuildmat.2019.07.319.
36. GB/T 17671-1999. 1999. Available from https://std.sacinfo.org.cn. [Accessed 2024].
37. Method for determination of fluidity of cement mortar. GB/T 2419-2004. 1999. Available from https://std.sacinfo.org.cn. [Accessed 2024].
38. GB/T 50082-2009. Standard for test methods of long-term performance and durability of ordinary concrete. Beijing: China Architecture & Building Press; 2009.
39. Luan C, Wu Z, Han Z, Gao X, Zhou Z, Du P, et al. The effects of calcium content of fly ash on hydration and microstructure of ultra-high performance concrete (UHPC). J Cleaner Prod. 2023;415(3):137735. doi:10.1016/j.jclepro.2023.137735.

40. Shen D, Liu C, Luo Y, Shao H, Zhou X, Bai S. Early-age autogenous shrinkage, tensile creep, and restrained cracking behavior of ultra-high-performance concrete incorporating polypropylene fibers. Cem Concr Compos. 2023;138(14):104948. doi:10.1016/j.cemconcomp.2023.104948.
41. Zhang B, Zhu H, Cheng Y, Huseien GF, Shah KW. Shrinkage mechanisms and shrinkage-mitigating strategies of alkali-activated slag composites: a critical review. Constr Build Mater. 2022;318:125993.
42. Wang R, Gao X. Relationship between flowability, entrapped air content and strength of UHPC mixtures containing different dosage of steel fiber. Appl Sci. 2016;6(8):216.
43. Huang H, Gao X, Zhang A. Numerical simulation and visualization of motion and orientation of steel fibers in UHPC under controlling flow condition. Constr Build Mater. 2019;199:624–36.
44. Chang PK, Hou WM. A study on the hydration properties of high performance slag concrete analyzed by SRA. Cem Concr Res. 2003;33(2):183–9.